CLM-P679

CLM-P679

UKAEA

Preprint

A COMPARISON BETWEEN LASER INDUCED FLUORESCENCE AT BALMER-ALPHA AND AT LYMAN-ALPHA FOR THE MEASUREMENT OF NEUTRAL HYDROGEN DENSITIES IN FUSION PLASMAS

P. GOHIL
D. D. BURGESS

CULHAM LABORATORY
Abingdon Oxfordshire
1982

CLM-P 679

A COMPARISON BETWEEN LASER INDUCED FLUORESCENCE AT BALMER-ALPHA AND AT LYMAN-ALPHA FOR THE MEASUREMENT OF NEUTRAL HYDROGEN DENSITIES IN FUSION PLASMAS

by

P Gohil* and D D Burgess*

Culham Laboratory, UKAEA, Abingdon, Oxon.

(Euratom/UKAEA Fusion Association)

ABSTRACT

This paper examines the relative merits of laser induced fluorescence scattering at the Lyman-alpha and Balmer-alpha wavelengths for the measurement of both the spatial distribution and absolute magnitude of neutral hydrogen densities in fusion plasmas. The enhancements of the fluorescence signals for present and for saturation laser intensities are determined and signal to noise ratios are presented for a range of fusion plasma conditions. Details of the interpretation of the fluorescence signals, and the limitations, at the two wavelengths are discussed. Balmer-alpha fluorescence scattering allows the measurement of neutral densities as low as $10^7 cm^{-3}$, whereas present intensities from Lyman-alpha sources permit fluorescence measurements only for neutral hydrogen densities approaching $10^{10} cm^{-3}$. Also presented is a technique for the spatial measurement of the electron number density based upon fluorescence scattering on the Balmer transitions, this process not being possible at Lyman-alpha for the range of electron densities in magnetically contained fusion plasmas. This may have applications in regions of the plasma otherwise difficult to diagnose, for example, near divertors and limiters.

*Blackett Laboratory, Imperial College of Science and Technology, London, SW7

(submitted for publication in Journal of Plasma Physics)

July, 1982

1. INTRODUCTION

Neutral hydrogen plays an important role in the energy and particle balance in magnetically contained fusion plasmas, since the neutrals are not constrained by the magnetic and electric fields present. Therefore, fast neutrals, produced in the plasma centre as a result of charge exchange between cold neutrals and energetic protons, may diffuse out to the plasma periphery, where further charge exchange and recycling may occur (Berry et al (1974), Izvozchikov and Petrov (1976), Duchs et al (1977)). At the vessel walls, impurities (Mo, W, C, O) may be released by the incidence of energetic neutrals (sputtering) or by evaporation or arcing (McCracken and Stott (1979), Roberto et al (1980)). High radiation fluxes produced by the impurities contribute towards the overall energy loss from the plasma. Between 50 and 85% of the total electron energy loss has been attributed to impurity radiation losses in PLT (Bol et al (1979)), and between 60% to 80% for ORMAK (Edmonds and England (1978)). Consequently, very large increases in the Lawson criteria result in increased fractions and high atomic number, Z, of the impurity ions (Jensen et al (1977), Piuatti et al (1981)).

The importance of neutral hydrogen with respect to the impurity ions arises from charge exchange recombination between the two species, resulting in lower ionization stages of the ion which then radiate strongly since the charge exchange mechanism preferentially produces highly excited states. Charge exchange recombination dominates over free electron recombination given that the ratio of neutral hydrogen density to the free electron density, n_H/n_e, is greater than 10^{-5} (Peacock, 1980). Therefore, plasma heating through high energy neutral beam injection (>20 keV) also results in substantial increases in the radiative losses by impurities (Hulse et al (1980), Suckewer et al (1980)).

In consequence considerable attention has been paid to schemes for accurate measurement of the neutral hydrogen density, n_H, in both the central and peripheral region of large magnetically contained fusion plasmas. This paper discusses the relative merits of two possible techniques based on laser-induced fluorescence scattering.

2. SPECTROSCOPIC POSSIBILITIES FOR MEASUREMENT OF NEUTRAL HYDROGEN CONCENTRATIONS.

In principle neutral densities can be inferred simply from Abel inversion of hydrogen line emission. However, detailed a-priori knowledge of the radial electron density, $n_e(r)$, and electron temperature, $T_e(r)$, profiles are required coupled with the use of a complete collisional-radiative calculation in order to relate the local emissivities to the total hydrogen concentration. The method is further complicated since the line emission is not uniform throughout the plasma, with the greatest contribution resulting from the plasma periphery, and radial symmetry in the emission may not be present. In addition geometrical constraints in large tokamak devices on the number of positions at which emission can be monitored severely limit the accuracy and scope of such Abel inverted techniques.

An alternative method of measuring the neutral densities is based upon resonant charge exchange between protons and neutrals, whereby neutrals incident at the plasma boundary are detected by an energy analyser (Barnett and Ray (1972), Petrov (1976)). However, this technique also requires extensive knowledge of $n_e(r)$ and $T_e(r)$ and also the transport of the neutrals from the centre of the plasma to the periphery has to be modelled (Berry et al (1974), Duchs et al (1977)).

Laser induced fluorescence scattering allows an accurate measurement of both the spatial and absolute magnitude of the neutral hydrogen to be made with minimal knowledge of the $T_e(r)$ and $n_e(r)$ profiles (Gohil, P., PhD Thesis, Univ of London, 1982). Furthermore, laser induced fluorescence offers possibilities of measuring:

(a) The ion temperature by scanning through the Doppler broadened atomic linewidth.
(b) The spatial concentration of impurity species. As an example, measurements of neutral Fe densities have been performed (eg Schweer et al (1980) and Muller and Burrell (1980)).
(c) The spatial electron density from the decay of the fluorescence after termination of the laser pulse.

An early attempt at measurement of neutral hydrogen by laser induced fluorescence was made (unsuccessfully) on the CLEO tokamak at Culham (Skinner, 1974). Since then successful measurements have been carried out on the FT-1 tokamak (Razdobarin et al, 1979) and the HBTXIA reverse field pinch (Gohil et al, 1982). In all these experiments, the probed transition was the visible Balmer-alpha line.

The use of laser induced fluorescence at the VUV Lyman-alpha transition (n=1 to n=2, λ = 1215Å) for the measurement of the neutral density has been proposed several times (Breton and Papoular (1975), Bogen and Lie (1978), Koopman et al (1978), Steuer and Wrobel (1978)). The main argument for working at Lyman-alpha (as opposed to fluorescence at the visible Balmer transitions, eg Balmer-alpha and Balmer-beta) is the substantial N_1^0/N_2^0 level population ratio present in high temperature fusion plasmas (for T_e = 1000 eV, $N_1^0/N_2^0 = 3.5 \times 10^3$ at $n_e = 5 \times 10^{12} cm^{-3}$ and N_1^0/N_2^0 = 55 at $n_e = 5 \times 10^{14} cm^{-3}$).

This apparent advantage of Lyman-alpha has led to work at several centres attempting to construct a coherent Lyman-alpha source of adequate intensity for fluorescence scattering observations on plasmas (Mahon and Yiu (1980), Steuer and Wrobel (1978)). However, past arguments in favour of Lyman-alpha have been rather unquantitative in their comparison (if any) with the possibilities of Balmer line scattering, and until the present paper no proper numerical comparison of the two techniques has ever been published. The main conclusion of the present paper is that a number of important considerations have been ignored in previous work and the real advantage actually lies heavily with the Balmer scattering approach.

3. COLLISIONAL-RADIATIVE MODEL FOR HYDROGEN

The interpretation of the magnitude and temporal behaviour of fluorescence signals during laser resonant pumping requires the investigation of the neutral hydrogen level populations prior to, during and after laser irradiation. This involves the modelling of the interaction of the hydrogen atomic level populations with respect to each other and the continuum, necessitating the detailed analysis of all the atomic processes occurring within the plasma region of interest.

In the present work the population N_i of the ith atomic level for non-laser irradiation was described by a set of rate equations corresponding to the standard collisional-radiative model (Bates et al (1962), Johnson and Hinnov (1973)):

$$\frac{dN_i}{dt} = \sum_{j=i+1}^{p} N_j A_{ji} + n_e \left[\sum_{\substack{j=1 \\ j\neq i}}^{p} N_j C_{ji} + n_e (U_i + C_{ci}) \right]$$

$$+ \sum_{j=p+1}^{p^*} N_j (n_e C_{ji} + A_{ji})$$

$$- N_i \left[\sum_{j=1}^{i-1} A_{ij} + n_e \left(\sum_{\substack{j=1 \\ j\neq i}}^{p^*} C_{ij} + C_{ic} \right) \right] + D_i \qquad (3.1)$$

where A_{ji} (sec^{-1}) are the spontaneous decay rates, C_{ij} and C_{ji} ($cm^3 s^{-1}$) are the collisional rate coefficients between level i and level j, C_{ic} and C_{ci} ($cm^3 s^{-1}$) are the collisional ionisation and recombination rates respectively, U_i ($cm^3 s^{-1}$) is the radiative recombination rate, D_i($cm^{-3} s^{-1}$) is the nett rate of atoms in level i diffusing into the volume of interest, and n_e is the electron density.

The inclusion of an infinite number of levels in Eqn 3.1 was avoided by taking level populations of states i, where $p < i < p^*$ ($p=20$, $p^*=50$), to be at LTE (ie Saha-Boltzmann densities) since these levels are strongly coupled, through the high collision rates, with each other and the continuum. The l and m sublevels of principal quantum level i were taken to be populated according to their statistical weights as a result of the high collision rates between the sublevels.

The plasma was assumed to be optically thin ($\tau < 1$) in the Lyman series given that the product Nd (where N is the neutral density (cm^{-3})

and d(cm) is the plasma dimension) was less than $1.8 \times 10^{14} cm^{-2}$ and $5.6 \times 10^{14} cm^{-2}$ at T_e = 100 eV and 1000 eV respectively.

The collision rates were obtained from the semi-empirical formulae of Johnson (1972). Although discrepancies between experimental results and theoretical predictions, using Johnson's rates, exist in low temperature, high density plasmas (T_e = 1 eV, $n_e = 10^{15} cm^{-3}$) (Burgess et al (1978), Burgess et al (1980)), the electron collision rates should be accurate at the high temperatures present in fusion plasmas, since the peak of the electron velocity distribution occurs well into the Born approximation limit to the excitation cross-sections. The radiative rates of Wiese et al (1966) and the radiative recombination rates of Seaton (1959) were used.

The rates Equation 3.1 can be expressed in matrix notation as:

$$\frac{d\underset{\sim}{N}}{dt} = \underset{\sim}{A}\,\underset{\sim}{N} - \underset{\sim}{X} \qquad (3.2)$$

where $\underset{\sim}{A}$ is the matrix (of order (pxp)) containing the rate coefficients linking the atomic levels, $\underset{\sim}{N}$ is the column vector (pxl) of level populations and $\underset{\sim}{X}$ is the column vector (pxl) of the recombination rates from the continuum and the higher levels (i > p).

For given plasma conditions, the collisional rate coefficients in matrices $\underset{\sim}{A}$ and $\underset{\sim}{X}$ are taken to be constant over the times of interest (eg during laser irradiation), which are short compared to the plasma lifetime and hence to the times in which n_e and T_e change.

Eqn 3.2 was solved for N_i by time iteration by using a method based on the divided-difference expression of Gear's method for the solution of 'stiff' equations (Gear (1971), Craigie (1974)). 'Stiff' equations contain many rapidly varying transients of different timescales in the solution. The solution was obtained by multi-stepping, whereby information from previous steps is used to define the present step length (Krogh, 1973). The stability and error in this method was controlled by defining an accuracy parameter, α, such that the error, $E_i(n)$, in the computed value of $N_i(n)$ at step, n, is given by:

$$\frac{E_i(n)}{N_i(n)} < \alpha \text{ for levels } i=1,2 \ldots..20$$

(α was typically 10^{-5}).

The level populations for neutral hydrogen were determined for a large range of n_e and T_e present in fusion plasmas. For these conditions the level populations, N_i,($i \geq 2$), arrive at equilibrium with the ground state in times on the order of nanoseconds, although the ground state itself relaxes to a steady state value in a timescale typically four to five orders of magnitude greater. Therefore, the local excited level populations (ie $i \geq 2$) assume quasi steady state values with respect to a given ground state density, n_H, and electron density, n_e, and temperature, T_e.

The level populations obtained by the present collisional-radiative code when run for quasi-steady conditions agree exactly with the values presented in Johnson and Hinnov (1973), who used the collision rates of Johnson (1972).

During laser irradiation, the rates matrix $\underset{\sim}{A}$ in Eqn 3.2 is modified by the presence of the time dependent laser induced rates, such that,

$$a_{ii}(t) = a_{ii}(t=0) - R^L_{ij}(t)$$

$$a_{ij}(t) = a_{ij}(t=0) + R^L_{ji}(t)$$

$$a_{ji}(t) = a_{ji}(t=0) + R^L_{ij}(t)$$

$$a_{jj}(t) = a_{jj}(t=0) - R^L_{ji}(t)$$

where, for instance, $a_{ii}(t)$ is the element in row i and column i in the time dependent matrix $\underset{\sim}{A}(t)$ containing the laser induced rate $R^L_{ij}(t)$, and $a_{ii}(t=0)$ is the matrix element prior to laser irradiation, and

$$R^L_{ji}(t) = \frac{\lambda^5_{ij}}{8\pi hc^2} A_{ji} I(\lambda,t)$$

and

$$R^{L}_{ij}(t) = \frac{g_j}{g_i} R^{L}_{ji}(t)$$

where R^{L}_{ij} and R^{L}_{ji} are the laser induced photoexcitation and stimulated emission rates respectively, $I(\lambda,t)$ is the laser intensity (per unit wavelength), λ_{ij} is the wavelength of the pumped transition, g_j and g_i are the statistical weights of levels j and i respectively.

The enhancements of the excited level populations as a result of optical pumping were calculated for various conditions with pump radiation applied on the Lyman-alpha and Balmer-alpha transitions. In the next sections, these results are used to obtain the requirements, limitations and sensitivities of fluorescence experiments in fusion plasmas.

4 LASER PUMPING REQUIREMENTS

During laser pumping at the saturation intensity, as defined below, for a specific transition:

(i) at infinite laser intensity the ratio of the population of the upper and lower pumped levels (j and i respectively) would tend towards the ratio of their respective statistical weights, ie

$$\frac{N_j}{N_i} = \frac{g_j}{g_i}$$

and for a given finite laser intensity the ratio becomes

$$\frac{N_j}{N_i} = F_s \frac{g_j}{g_i}$$

where F_s can be defined as the saturation factor (F_s lies between 0 and 1).

(ii) the greatest possible enhancement of the upper level populations is produced for F_s approaching unity.

Also, for laser intensities above the saturation intensity, the behaviour of the upper level population, N_j, becomes independent of the laser intensity. Interpretation of the fluorescence signal then requires no knowledge of the absolute laser pump intensity at the observed irradiated volume and time integration of the signals is independent of the temporal variation in the laser intensity.

The laser intensity, I_s^λ, into 4π (assumed constant across the line profile) required to saturate a given transition of wavelength, λ, is given by:

$$I_s^\lambda = \frac{8\pi hc^2}{\lambda^5} \frac{1}{A_{ji}} \frac{F_s}{1-F_s} \left[(X_{ji} + X_j + A_{ji}) - \frac{g_i}{g_j} X_{ij} \right]$$

$$\text{Watts cm}^{-2}\ \text{Å}^{-1}$$

where A_{ji} is the radiative transition rate (sec^{-1}); X_{ji} and X_{ij} are the collisional de-excitation and excitation rates (sec^{-1}) respectively between the levels i and j; X_j is the total collisional rate (sec^{-1}) out of level j to higher lying levels. In the present context, the saturation intensity cannot be achieved simply by focussing down to a small laser spot size because of limitations (discussed below) set by background emission. For practical purposes, the minimum laser spot size is about 1 cm^2, and this value is assumed in calculating the power densities below.

Figure 1 shows the laser intensities required to saturate the Balmer-alpha and Lyman-alpha transitions as a function of the electron number density, n_e, at various electron temperatures, T_e. The laser linewidth in each case is taken to be 1.5 times the Doppler width. The value of F_s for both the Balmer-alpha and Lyman-alpha transitions is taken to be 0.5 (ie 50% saturation). Also indicated in Fig. 1 is the highest Lyman-alpha power density reported to date (Mahon et al (1978), Cotter (1979), Mahon and Yiu (1980)) which is seen to be still three orders of magnitude less than that needed to saturate the Lyman-alpha transition. In the case of Balmer-alpha lasers, powers of 1 MW are readily available using flashlamp pumped dye lasers.

For both the Lyman-alpha and Balmer-alpha transitions in fusion plasmas the atomic linewidth is predominantly Doppler broadened. For Balmer-alpha the FWHM Doppler widths, $\Delta\lambda_D$, at T_e = 100 and 1000 eV are 5.0 and 16.0 Å respectively, while for Lyman-alpha the FWHM Doppler widths at the same temperatures are 1.0 and 3.1 Å respectively.

Since Doppler broadening is inhomogeneous, the greatest fluorescence signal is obtained for $\Delta\lambda_L > \Delta\lambda_D$, where $\Delta\lambda_L$ is the laser linewidth. This requirement is easily satisfied by Balmer-alpha lasers at T_e = 1000 eV (assuming $T_e = T_H$), but for Lyman-alpha lasers the power density required to saturate at T_e = 1000 eV would be greater than 2 MW cm^{-2}. This value is over 4000 times greater than that available from present sources of coherent Lyman-alpha radiation.

5. POPULATION ENHANCEMENT

The behaviour of the populations of the upper levels resulting from laser pumping were determined by using the time dependent multi-level collisional-radiative model for hydrogen. The parameters of interest are the absolute enhancement, ΔN_j, which determines the signal level and the relative enhancement, N_j^L/N_j^0, which determines the signal/background emission ratio and hence, in practice, the signal to noise ratio.

Figure 2 shows the peak of the increased n=2 level population as a function of the Lyman-alpha laser power density. Also shown is the peak population expected with presently available Lyman-alpha laser power densities, for the case of the whole Doppler width being pumped.

In the latter case, the resultant peak population lies well in the linear region of growth of N_2^{Peak} with increasing laser power density. Therefore, for the determination of the n=1 level population from the Lyman-alpha fluorescence signal, knowledge of the laser energy at the scattering volume, after transmission through the input optics, is then required and (unlike the saturated case feasible at Balmer-alpha) the scattered signal is sensitive to laser intensity fluctuations (eg shot-to-shot). On the other hand, detailed knowledge of the spatial variation of the laser intensity at the scattering volume is not essential provided that the Lyman-alpha laser intensity remains within the low intensity linear region indicated in Fig. 2. However, the

signal to noise values obtained with Lyman-alpha irradiation are then very poor (see Fig. 7). If higher Lyman-alpha intensities become available the exact spatial intensity distribution will have to be accurately known (on each shot) if the illuminating intensities lie in the non-linear region (ie between 50 and 500 kW $cm^{-2}Å^{-1}$). Outputs exceeding 500 kW will be needed before Lyman-alpha systems can provide the great practical advantage of saturation already easily available at Balmer-alpha. Furthermore, given the present inability to saturate at Lyman-alpha, increasing the irradiating volume does not produce any increase in the scattered Lyman-alpha fluorescence signal relative to background emission. For Balmer-alpha, however, signal to background values can be substantially increased by increasing the laser spot size at the expense of a modest loss of spatial resolution (whilst still retaining the advantages of saturation).

Figure 3 shows the computed ratio of N_2^{Peak}/N_2^0 resulting from Lyman-alpha lasers operating at the saturation intensity and at presently available intensities as a function of the electron number density, n_e. The decrease in the N_2^{Peak}/N_2^0 ratio with increasing n_e results because the initial population, N_2^0, increases with n_e due to the increased collision rate, X_{12}, populating n=2 from n=1. This behaviour is reflected in a decreasing signal-to-noise ratio of the fluorescence signal with increasing n_e, as will be shown later. The relative enhancement of the n=2 level population, obtained at present Lyman-alpha intensities, quickly decreases below a value of unity for $n_e > 5 \times 10^{13} cm^{-3}$.

In contrast, Fig. 4 shows how the computed ratio of N_3^{Peak}/N_3^0 varies during laser irradiation at the Balmer-alpha wavelength and at saturation intensity. There is no marked variation in the ratio with the electron density, n_e, since the relative increases in the initial populations of n=2 and n=3 are very similar to each other because of the strong coupling of the lower lying excited levels (ie n=2, n=3, n=4) to the ground state. Furthermore, the ratio N_3^{Peak}/N_3^0 is insensitive to the electron temperature, T_e, because the mean energy of the free electrons is much greater than:

(i) the energy difference between the excited levels and

(ii) the ionization energies of the levels.

However, the change in the absolute population, ΔN_3, of the n=3 level increases with n_e since the initial lower level population, N_2^0, also increases with n_e. Figure 5 indicates how ΔN_3 behaves as a function of the ground state (n=1) population at several electron number densities. The linear dependence of ΔN_3 on the n=1 level population results from the fact that the initial level population, N_2^0, of n=2 is very strongly coupled to that of the n=1 level. The only departure from a linear relationship occurs at high electron densities and low n=1 population densities, when the total collision rates linking n=2 and n=1 are similar in magnitude to the total collision rates coupling n=2 to the higher levels and the continuum. In conclusion, interpretation of the ground state density from the absolute enhancement of the Balmer-alpha fluorescence signal is then less ambiguous than would be the case for a Lyman-alpha signal obtained at irradiating intensities below the saturation requirement.

6. PREDICTED SIGNAL-TO-NOISE RATIOS IN PRACTICAL EXPERIMENTAL SITUATIONS AND IMPLICATIONS FOR SPATIAL RESOLUTION

Figure 6 shows a typical experimental layout for a fluorescence experiment.

The number of photoelectrons, F_N, produced by the detection system as a result of laser pumping for time duration, T_L, is given by:

$$F_N = \eta\, A_{ji} V_F \frac{\Delta\Omega}{4\pi} \int_0^{T_L} [N_j(t,r) - N_j(o,r)]\, dt$$

where N_j (t,r) is the level population of the upper level, j, at time, t, (after laser initiation) and radial position, r, from the centre of the plasma: T_L is the laser duration: η is the overall efficiency of the detection system: A_{ji} is the spontaneous decay rate from the upper level, j: $V_F(cm^3)$ is the laser irradiated volume as observed through the detection optics: and $\Delta\Omega$ (sr) is the detection solid angle. However, the detection of the local laser induced fluorescence signal is limited by the extent of background fluorescence also observed by

the detection optics. The number of photoelectrons, B_N, produced by the background fluorescence is:

$$B_N = \eta\, A_{ji}\, \frac{\Delta\Omega}{4\pi}\, 2r_L L \int_0^{T_L} \int_{-r_T}^{r_T} N_j^0(o,r)\, dr\, dt$$

Assuming that shot noise dominates, the signal-to-noise ratio is given by:

$$S/N = \frac{F_N}{(F_N + B_N)^{\frac{1}{2}}} = \sqrt{K(\lambda)\, T_L}\ \left(\frac{V_F \Delta N_j}{[V_F \Delta N_j + 1.5\, V_B N_j^O]^{\frac{1}{2}}} \right)$$

where $K(\lambda) = \eta\, A_{ji}\, \frac{\Delta\Omega}{4\pi}$
and $V_B = 4r_L L r_T$ = background volume. (Note that whereas a balanced detector system as used by Razdobarin et al (1979) can remove the background signal, it does not improve the above signal to noise ratio).

Detailed modelling of the edge regions of the plasma is not required because the large difference in Doppler width between the hot centre and cooler edge regions means that emission from the cold neutrals at the edge of the plasma can be spectrally filtered out, and thus does not contribute to the effective background. Since emission and fluorescence from the hot neutrals in the plasma centre, typically, will have a Doppler width a factor of ten or more greater than that of the cold edge neutrals the plasma centre fluorescence can be detected in this manner without significant loss of signal. Therefore, for observations of neutral hydrogen in the plasma centre the background signal can be assumed to essentially consist only of emission from neutrals corresponding to the same plasma conditions as present in the fluorescing volume. Correspondingly, the signal to noise will be basically limited by the ratio of the laser irradiated fluorescing volume to the background volume as observed by the detection optics, rather than by any plasma boundary effects.

The factor 1.5 takes into account an assumed slight increase in the initial level populations near the plasma periphery before the Doppler temperature actually drops. Since the fluorescence signal saturates and becomes independent of increased laser intensities above the saturation intensity (in contrast to Thomson scattering), any further increase in the fluorescence signal can then only be produced by increasing the laser irradiated volume or the laser pulse duration.

In the case of Balmer-alpha, taking η = 5%, $\Delta\Omega = 2 \times 10^{-3}$ Sr (ie a lens of diameter 5 cm and distance 100 cm from the plasma), $A_{32} = 4.4 \times 10^{7} s^{-1}$, then K(Balmer-alpha) is 350. For Lyman-alpha, taking η = 0.5% (which results from the low transmission characteristics of the LiF optics (50%) and Lyman-alpha filters (15%)), $\Delta\Omega = 2 \times 10^{-3}$Sr, $A_{21} = 4.7 \times 10^{8}\ s^{-1}$, then K(Lyman-alpha) = 374.

Figure 7 shows how the S/N ratio for Lyman-alpha and Balmer-alpha varies with the electron number density, n_e. The quantities used were:

(i) a background volume 100 cm^3

(ii) laser duration of 2 μs and 10 ns for the Balmer-alpha and Lyman-alpha lasers respectively.

(iii) scattering volumes of 1 cm^3 for both the Balmer-alpha and Lyman-alpha wavelength cases. Also shown is the increase in the S/N ratio possible for Balmer-alpha as a result of pumping and observing a larger irradiated volume (eg for V_F = 5 cm^3). This is possible in the case of Balmer-alpha because of the ease of increasing the scattering volume whilst still being able to maintain a saturating laser flux. Attempts to do likewise with Lyman-alpha lasers would require powers of greater than 3 MW. (Increasing the scattering volume with present Lyman-alpha systems operating well below saturating intensity of course produces no increase in the signal).

(iv) a ground state density of $10^{10} cm^{-3}$.

The Balmer-alpha signal-to-noise ratio exceeds that of Lyman-alpha at high electron densities because the N_2^0/N_1^0 ratio increases with n_e, which results in a larger background fluorescence flux at Lyman-

alpha, but a larger laser induced fluorescence signal in the case of Balmer-alpha.

In comparison, as shown in Fig. 7, the S/N ratio with presently available Lyman-alpha laser powers (500 Watts) is below that for Balmer-alpha at saturation intensities.

By increasing the scattering volume and the laser duration, the sensitivity of the fluorescence measurement can be improved. Figure 8 shows the minimum resolvable n=1 level population using Balmer-alpha fluorescence for various scattering volumes and laser durations at $n_e = 10^{13} cm^{-3}$ and T_e = 100 eV and 1000 eV. K(Balmer-alpha) is 350 and the background volume is taken to be 100 cm^3. (The S/N ratio corresponding to the minimum resolvable density is taken to be 2).

Figure 9 shows the minimum resolvable ground state density at $n_e = 10^{14} cm^{-3}$ and T_e = 100 eV and 1000 eV. The sensitivity improves at the higher electron density because of the resulting higher N_2^0 population which produces a greater ΔN_3 value during laser irradiation. The reduction in sensitivity at high electron temperatures, T_e = 1000 eV, results from a lower N_2^0 value arising from the decreased collision rate, X_{12}, since the peak of the velocity distribution has moved further into the high energy region where the Born-approximation should be adequate.

With present Lyman-alpha laser powers, the minimum resolvable n=1 density is $9 \times 10^9 cm^{-3}$ which would probably only allow for a successful measurement of the neutrals in the extreme boundary region.

7. INTERPRETATION OF THE FLUORESCENCE SIGNAL

For Lyman-alpha laser intensities below the saturation intensity, exact details are required of the laser energy at the region of the observed laser irradiated volume for the determination of the ground state density. The scattered signal will be sensitive to shot to shot fluctuations in laser output. The transmission of the LiF optics deteriorates as a result of the influence of soft X-rays (Long et al, 1968) and even greater deterioration will in all probability be produced by the incidence of the neutron and alpha particle flux in the larger machines eg such as JET. Furthermore, the scattered fluorescence signal will be greatly reduced on transmission through the optics, so making the evaluation of the number of scatterers in the

observed volume very difficult, especially with a window transmission characteristic which may vary due to irradiation damage.

In the case of Balmer-alpha fluorescence, interpretation of the fluorescence signal is only limited by the knowledge of the local electron density at the observed volume. The scattered signal will be essentially independent of laser output fluctuations. The ability to saturate the Balmer-alpha transition allows for accurate time integration of the fluorescence signal which, together with increased scattering volumes, makes possible the determination of neutral hydrogen densities below $10^7 cm^{-3}$.

Although the use of interference filters at Lyman-alpha allows for larger detection solid angles than for slit-width limited VUV spectrometers, present Lyman-alpha filters have bandwidths of about 100Å. Problems might then occur due to the detection of several strongly radiating impurity lines (eg CIII (1175Å), NV (1239Å)). For example, in the TFR tokamak, the radiance of NV is more than 10 times greater than that of Lyman-alpha (Equipe TFR, 1975). This line could be reduced with the use of an oxygen cell, since oxygen has a minimum of absorption at Lyman-alpha, but this would further reduce the overall detection efficiency.

Proton collisions and non-resonant charge exchange, which selectively excite electrons from the 1s to 2s and 2p levels, will become important at T_e > 2 keV. (These processes were neglected in the Lyman-alpha analysis of Koopman et al (1978)). For example, non-resonant charge exchange between a ground state hydrogen atom and a proton, so producing an excited atom in the n=2 state, has a rate of between $10^7 - 10^8\ s^{-1}$ for an electron density range of $10^{13} - 10^{14} cm^{-3}$ and electron temperature between 2 and 5.5 keV. These processes will further reduce the N_1^0/N_2^0 population ratio, so producing a lower Lyman-alpha enhancement, but, in contrast, increasing the Balmer-alpha enhancement.

8. CONCLUSIONS

The following points arise in performing a laser induced fluorescence experiment in a fusion plasma at the Lyman-alpha and Balmer-alpha transitions:

(1) Since present Lyman-alpha laser intensities are about three orders of magnitude below the saturation intensity, the interpretation of the Lyman-alpha fluorescence signal becomes difficult and demands detailed knowledge of the laser energy at the scattering volume in the plasma. This procedure is not required in the case of Balmer-alpha fluorescence, where the ability to saturate the transition produces a signal which is independent of the laser intensity.

(2) The long pulse durations produced by Balmer-alpha lasers allow for improved signal to noise ratios through time integration of the fluorescence signal. This factor has been ignored in most previous comparisons, but is sufficient to allow usable signal to noise ratios to be obtained on Balmer-alpha. Furthermore, the signal is independent of the temporal behaviour of the laser intensity above the saturation intensity, so allowing for simple interpretation. Also, given the higher efficiencies of the detection system at Balmer-alpha, neutral hydrogen densities below $10^7 cm^{-3}$ can be measured, in contrast to the situation for Lyman-alpha lasers, where the minimum resolvable density is $9 \times 10^9 cm^{-3}$ at present intensities.

(3) Deterioration in the transmission of LiF windows through damage by not only X-rays, but also by neutron and alpha particles, poses severe interpretative problems for Lyman-alpha fluorescence observations (given also the inability to saturate). From a practical standpoint, it is worth noting that handling of the input beam, possibly over long distances, and, in the case of devices such as JET, through biological shields, is also very much easier at Balmer rather than Lyman line wavelengths.

(4) Although saturation of the Balmer-alpha fluorescence allows no further gain by increasing the laser intensity, the ability to saturate large volumes of the plasma with presently available visible flashlamp pumped dye lasers produces substantial improvements in the signal to noise ratios and hence the sensitivity without undue loss of spatial resolution.

(5) The n=2 and 3 levels are strongly coupled to the ground state through the electron collision rates at these high temperatures, so making the deduction of the ground state population from the Balmer-

alpha fluorescence signal straightforward. Furthermore, the fluorescence is insensitive to the electron temperature. The Lyman-alpha fluorescence is also insensitive to the electron temperature, but suffers from interpretative problems resulting from an inadequate pump intensity, even though the ground state is being probed directly.

(6) Finally, Balmer line scattering offers an extra diagnostic possibility. The electron density can be deduced (simultaneously with the neutral density) from observations of the decay of the fluorescence on the Balmer transitions after rapid termination of the laser pulse. The decay, for an appropriately chosen transition, will be collisionally dominated. Electron densities in the range 9×10^{12} to $10^{14} cm^{-3}$ can be spatially resolved by appropriately probing on the Balmer-alpha or Balmer-beta lines, see Fig. 10. This possibility is not available at Lyman-alpha until much higher values of n_e are reached. The possibility of n_H and n_e measurement may be useful in regions of the plasma otherwise difficult to diagnose, eg near limiters and divertors.

ACKNOWLEDGEMENTS

The authors would like to acknowledge many useful conversations with Drs N J Peacock and M J Forrest concerning diagnostic problems in large fusion devices.

P Gohil acknowledges support from UKAEA, Culham and SERC in the form of a CASE studentship.

REFERENCES

Barnett, C F & Ray, J A (1972) Nuc Fus 12, 65.

Bates, D R, Kingston, A E & McWhirter, R W P (1962) Proc Roy Soc A267,297.

Berry, L A, Clark, J F & Hogan, J T (1974) Phys Rev Lett 32, 362.

Bogen, P & Lie, Y T, (1980) J Nuc Mat 93 and 94, 363.

Bol, K, Arunasalam, V, Bitter, M, Boyd, D, Brau, K et al (1979) Proc 7th Int Conf on Plasma Physics and Controlled Nuclear Research, Vol 1, IAEA, Vienna, 11.

Breton, C S and Papoular, R (1975), Plasma Phys 15, 809.

Burgess, D D, Kolbe G & Ward, J M (1978), J Phys B 11 2765.

Burgess, D D, Myerscough, V, Skinner, C H & Ward, J M (1980) J Phys B 13, 1675.

Cotter, D (1979) Opt Comm 31, 397.

Craigie, J A I (1975), Num Anal Rep, Univ of Manchester, 11.

Duchs, D F, Post D E & Rutherford, P H (1977) Nuc Fus 17, 565.

Edmonds, P H & England, A C (1978) Nuc Fus 18, 23.

Equipe TFR (1975) Nuc Fus 15, 1053.

Gear, C W (1971) Comm.ACM 14, 176.

Gohil, P (1982), PhD Thesis, Univ of London.

Gohil, P, Kolbe, G, Forrest, M J, Burgess, D D & Hu, B Z (1982) Culham Preprint, CLM-P669.

Hulse, R A, Post, D E & Mikkelsen, D R (1980) J Phys B 13, 3895.

Izvozchikov, A B & Petrov, M P (1976) Sov J Plasma Phys 2, 117.

Jensen, R V, Post, D E, Grasberger, W H, Tarter, C B & Lokke, W A (1977) Nuc Fus 17, 1187.

Johnson, L C (1972) Astrophys J 174, 227.

Johnson, L & Hinnov, E (1973), JQSRT 13, 333.

Koopman, D W, McIlrath, T J & Myerscough, V (1978) JQSRT, 19, 555.

Krogh, F T (1973), SIAM J Num.Anal 10, 949.

Long, R C, Cox, D M & Smith, S J (1968), J Res.NBS 72A, 521.

Mahon R, McIlrath, T J & Myerscough, V (1978) App Phys Lett 33, 305.

Mahon, R & Yiu, Y M (1980), Opt Lett 5, 279.

McCracken, G M & Stott, D E (1979) Nuc Fus 19, 889.

Muller C H & Burrell K H (1980), General Atomic Preprint GA-A15806, General Atomic, San Diego.

Peacock, N J (1980) Culham Lab Report, CLM-P619.

Petrov , M P (1976) Fiz.Plazmy, 2, 371.

Piuatti, M E, Bretan, C, De Michelis, C, Mattioli, M (1981), Euratom-CEA Report, Eur-CEA-FC 1085.

Razdobarin, G J, Semenov, V V, Sokolova, L V, Folomkin, I P, Burakov, V S, Misakov, P Ya, Naumenkov,, P A & Nechaev, S V (1979) Nuc Fus 19, 1439.

Roberto, J B, Zuhr, R A & Withrow, S P (1980) J Nuc Mat 93-94, 127.

Schweer, B, Rusboldt, D, Hintz, E, Roberto, J B & Husinksky, J (1980) J Nuc Mat 93-94, 357.

Seaton, M, (1959) MNRAS 119, 90.

Skinner, C H (1974) PhD Thesis, University of London.

Steuer, K H & Wrobel, W G (1978), Max-Planck Institut Rep IPP 1/168.

Suckewer, S, Hinnov, E, Bitter, M, Hulse, R & Post, D (1980), Phys Rev A 22, 725.

Wiese, W C, Smith, M W & Glennon, B M (1966), Atomic Transition Probabilities, Vol 1 (US Dept of Commerce, 1966).

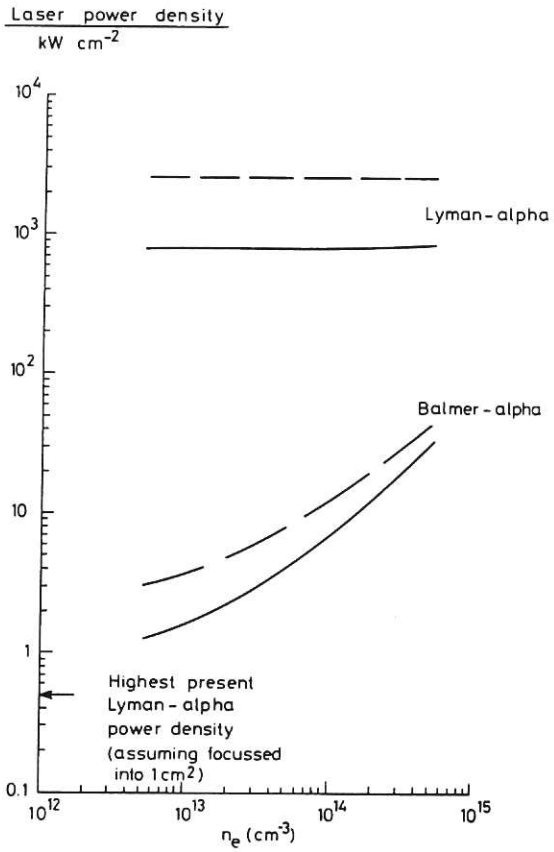

Fig.1 Laser power densities required to saturate the Lyman-alpha and Balmer-alpha transitions as a function of the electron number density.
($F_s = 0.5$, i.e. 50% saturation).
(laser linewidth = 1.5 × Doppler width)
——— $T_e = 100$eV. — — $T_e = 1000$eV.

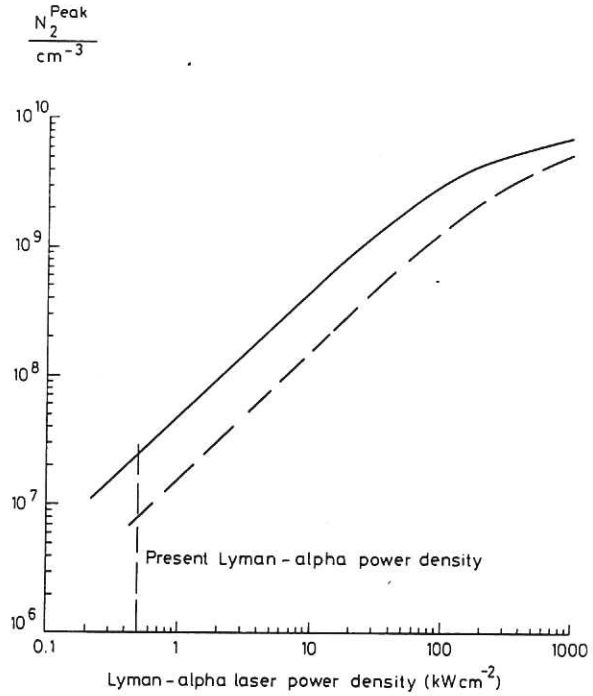

Fig.2 N_2^{Peak} as a function of the laser power density.
($N_1 = 10^{10}$ cm^{-3}; $n_e = 10^{13}$ cm^{-3})
——— $T_e = 100$eV
— — $T_e = 1000$eV.

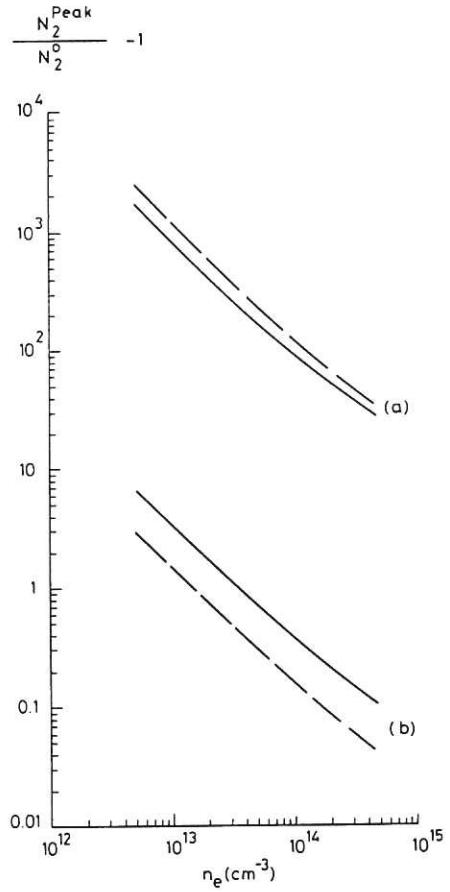

Fig.3 Relative population ratio, $[N_2^{Peak}/N_2^0 - 1]$, as a function of the electron number density ($N_1 = 10^{10}$ cm^{-3}).
(a) Saturation Power Density
(b) Presently available Power Density.
——— $T_e = 100$eV. — — $T_e = 1000$eV.

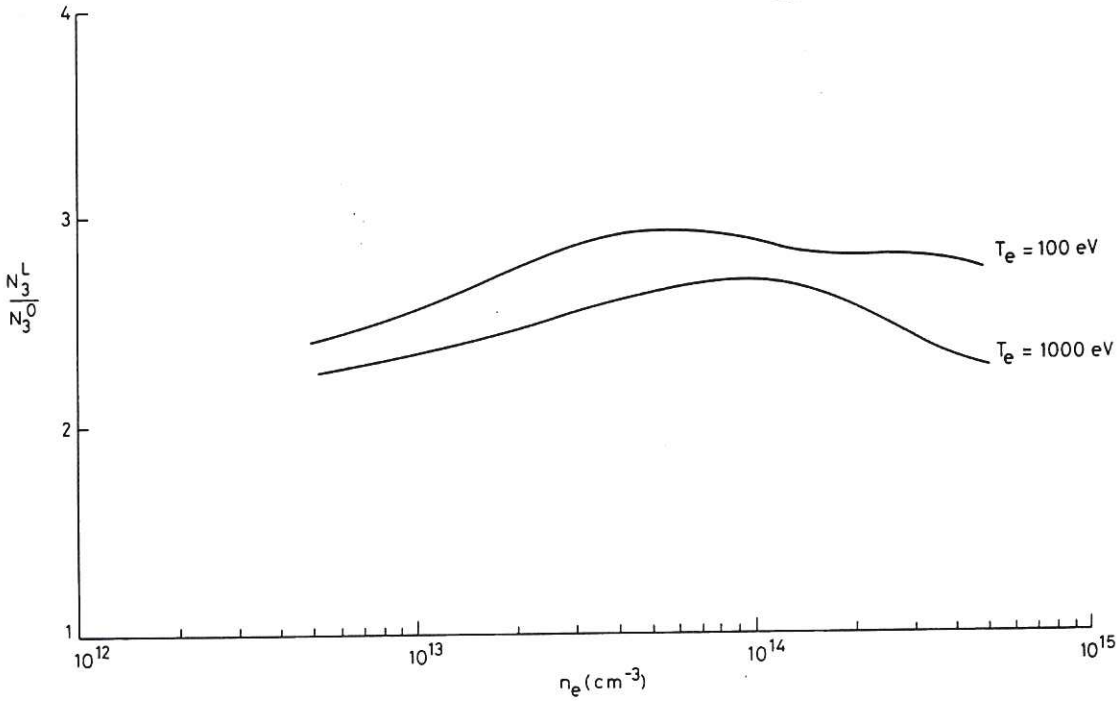

Fig.4 Ratio of peak laser irradiated N=3 population to initial population v. electron number density at various temperatures. ($N_1 = 10^{10}$ cm^{-3}).

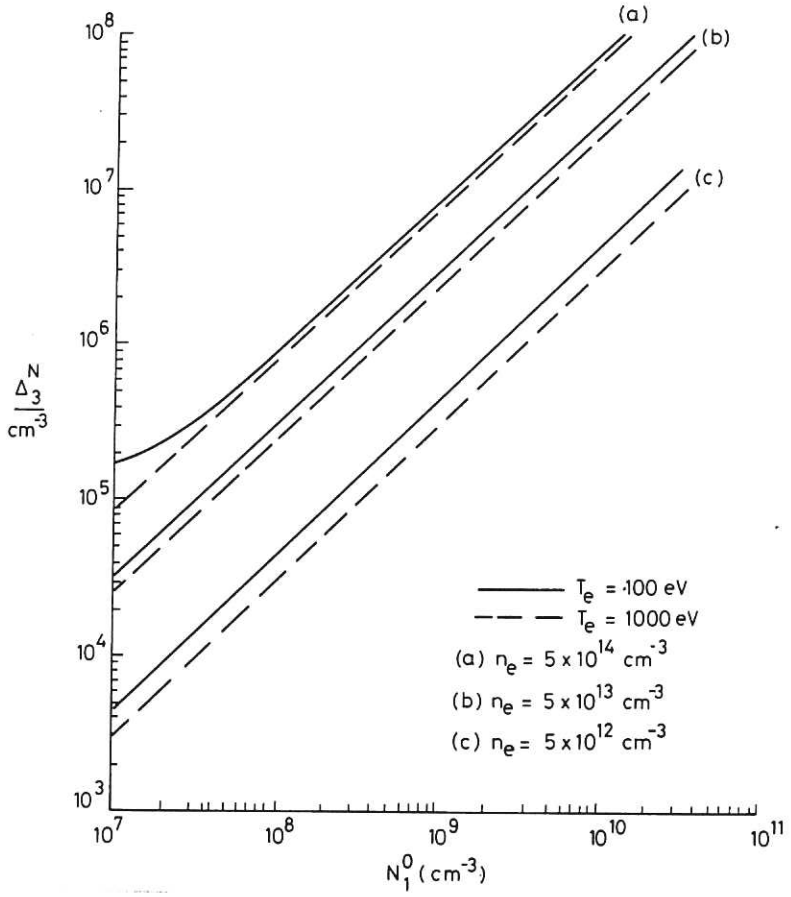

Fig.5 Increase in the n=3 level population, ΔN_3, during Balmer-alpha pumping as a function of the ground state density at various electron densities and temperatures.

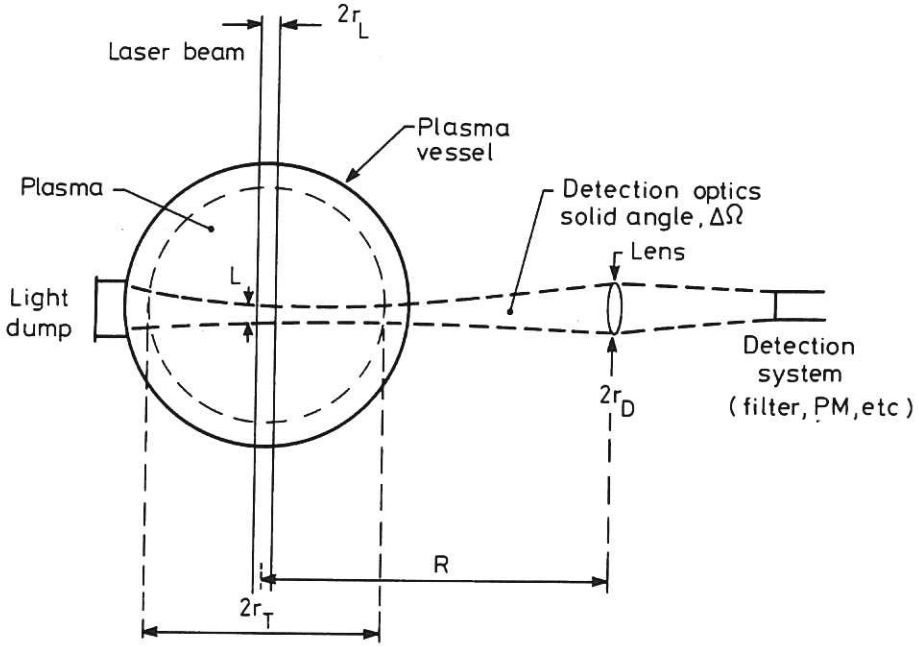

Fig.6 Experimental Layout for Fluorescence Detection.

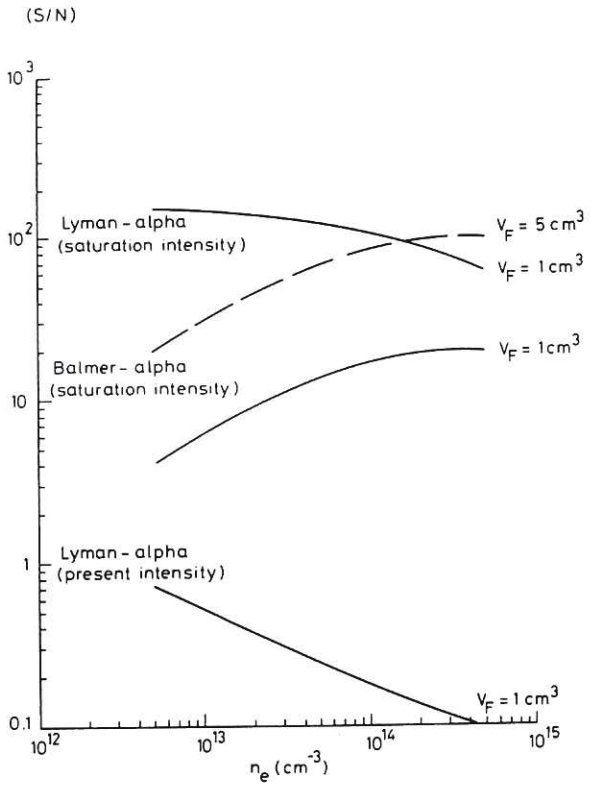

Fig.7 Signal-to-noise ratios for Lyman-alpha and Balmer-alpha laser pumping as a function of the electron number density. ($N_1 = 10^{10}$ cm^{-3}; T_e = 1000 eV). For Balmer-alpha: $T_L = 2\mu s$; V_F = 1 cm^3 and 5 cm^3.
Lyman-alpha: T_L = 10 ns; V_F = 1 cm^3.

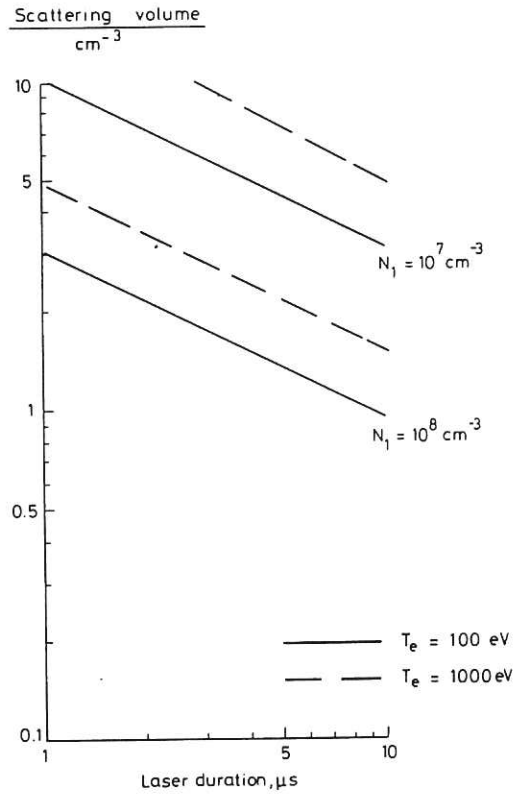

Fig.8 The minimum N_1 density resolvable from Balmer-alpha fluorescence as a function of scattering volume, V_F, and laser duration, T_L. ($n_e = 10^{13}$ cm^{-3}).

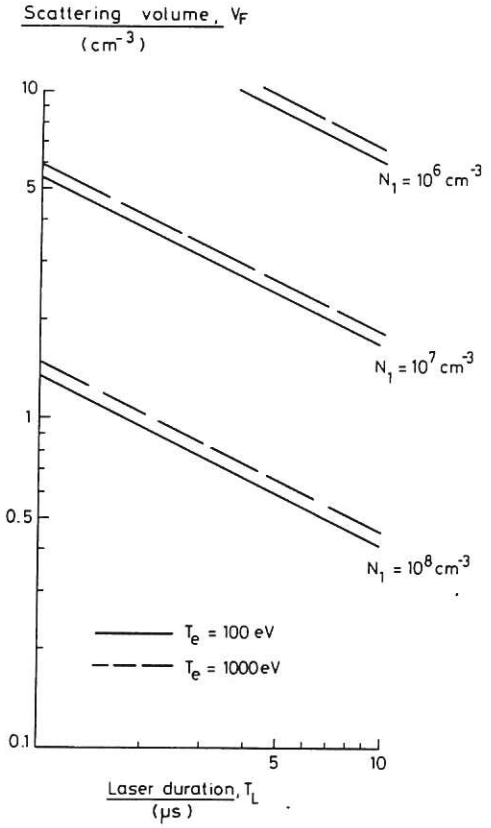

Fig.9 Minimum N_1 density resolvable from Balmer-alpha fluorescence as a function of the scattering volume, V_F, and laser duration, T_L, ($n_e = 10^{14}$ cm^{-3}).

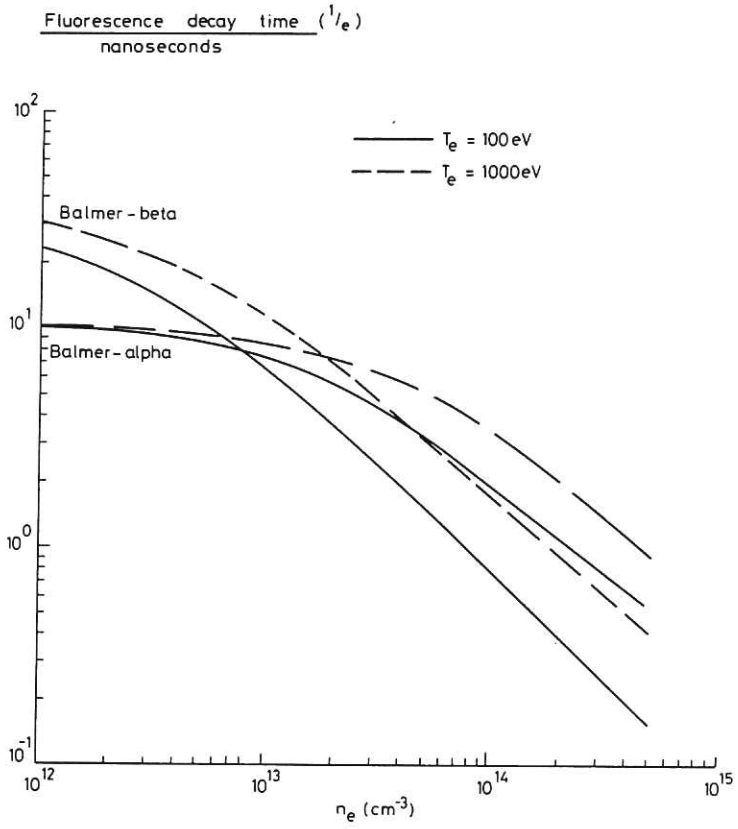

Fig.10 Decay time (1/e) of Balmer-alpha and Balmer-beta fluorescence as a function of the electron number density.